Pan et al. Nanoscale Research Letters (2015) 10:131
DOI 10.1186/s11671-015-0829-z

Nanoscale Research Letters
a SpringerOpen Journal

NANO EXPRESS Open Access

A novel method to fabricate $CoFe_2O_4/SrFe_{12}O_{19}$ composite ferrite nanofibers with enhanced exchange coupling effect

Lining Pan, Derang Cao, Panpan Jing, Jianbo Wang and Qingfang Liu*

Abstract

Nanocomposite of $CoFe_2O_4/SrFe_{12}O_{19}$ has been synthesized by the electrospinning and calcination process. A novel method that cobalt powder was used to replace traditional cobalt salt in the precursor sol-gel for electrospinning was proposed. The crystal structures, morphologies, and magnetic properties of these samples have been characterized in detail. Moreover, when the average crystallite size of the hard/soft phases reached up to an optimal value, the $CoFe_2O_4$ have an enhanced saturation magnetization of 62.8 emu/g and a coercivity of 2,290 Oe. Significantly, the hysteresis loops for the nanocomposites show a single-phase magnetization behavior, and it has been found that the exchange coupling interaction strongly exists in the $CoFe_2O_4/SrFe_{12}O_{19}$ magnetic nanocomposite nanofibers.

Keywords: Cobalt powder; $CoFe_2O_4/SrFe_{12}O_{19}$ nanocomposite nanofibers; Exchange coupling interaction; Crystallite size

Background

Cobalt ferrite ($CoFe_2O_4$) has attracted enormous concern due to its significant properties such as remarkable chemical and thermal stabilities, good mechanical hardness, and high saturation magnetization (M_s). They have been widely applied in diverse fields, including magnetic resonance imaging, magnetically targeted drug, permanent magnets, microwave absorption, and magnetic data storage [1-4]. Recently, a number of studies about the synthesis of $CoFe_2O_4$ have been reported. $CoFe_2O_4$ nanoparticles were fabricated by a sol-gel method by Xi et al. [5], Mazario fabricated the $CoFe_2O_4$ ferrite nanoparticles by an electrochemical method [6], $CoFe_2O_4$ nanofibers was obtained by the electrospinning in 2009 [7], Liu et al. prepared the $CoFe_2O_4$ nanoplatelets using a facile hydrothermal route [8], and so on. However, the applications of $CoFe_2O_4$ are often limited by its relatively low coercivity (H_c). The multitudinous experimental results show that the H_c could be improved drastically combining $CoFe_2O_4$ with hard ferrites to form nanocomposite via exchange coupling effect [9-14]. Among the hard ferrites, strontium hexaferrite ($SrFe_{12}O_{19}$) has significant performances such as high Curie temperature (T_c), high M_s, high H_c, large magnetocrystalline anisotropy (H_k), and excellent chemical stability [15-17]. So far, the growing efforts have been devoted to the investigation of nanocomposites of $CoFe_2O_4/SrFe_{12}O_{19}$ [18,19]. Nevertheless, these investigations indicated the presence of impurities such as α-Fe_2O_3 [19,20], which exhibited a twisted hysteresis loop and an incomplete exchange coupling between the hard and soft phases [9,13]. Furthermore, the presence of incomplete exchange coupling behavior severely leads to the decrease of magnetic properties. It is important to obtain the samples with no impurities and strong exchange coupling interaction. Compared with the former methods, electrospinning has been certified to be a simple, low-cost, and versatile technique capable of generating numerous one-dimensional (1D) nanostructures. As one of the typical 1D nanostructures, nanofibers have high surface-to-volume ratio, high aspect ratio, and big shape anisotropy compared to nanoparticle and bulk

* Correspondence: liuqf@lzu.edu.cn
Key Laboratory for Magnetic and Magnetic Materials of the Ministry of Education, Lanzhou University, Lanzhou 730000, People's Republic of China

[19,20]. Therefore, plenty of interests have been focused on the nanofibers because of their novel properties and potential applications [11,21].

Originally, when the cobalt salt was used in the synthetic process, cobalt ion replaces easily Fe or Sr ion or both in the $SrFe_{12}O_{19}$ [22]. Because the substitution between the ions leads to the destruction of the ratio of solution, the α-Fe_2O_3, $SrFe_2O_4$, and other impurity phases are easy to form. And to avoid the substitution, we proposed a novel way that cobalt powder was used in the precursor sol-gel to form a suspending liquid for electrospinning. In this work, the $CoFe_2O_4/SrFe_{12}O_{19}$ nanofibers were obtained by electrospinning followed by heating treatment. And the structure, chemical component, and magnetic properties were characterized in detail. The hard/soft phases contacted closer sufficiently than traditional composite particles and previous nanofibers, and the crystallite size of the two phases also achieved an optimal value, which lead to a strong exchange coupling.

Methods

In this work, $CoFe_2O_4$/ $SrFe_{12}O_{19}$ composite nanofibres were synthesized by electrospinning combined with the sol-gel technique. All chemical reagents were of chemical grade. As shown in Figure 1, in the typical synthesis, 1.2 mmol $Fe(NO_3)_3 \cdot 9H_2O$ and 0.1 mmol $Sr(NO_3)_2$ were dissolved together in a mixed solvent of 0.5 ml deionized water, 1.0 ml *N*,*N*-dimethylformamide (DMF), and 2.5 ml ethanol (C_2H_5OH), and then followed by magnetic

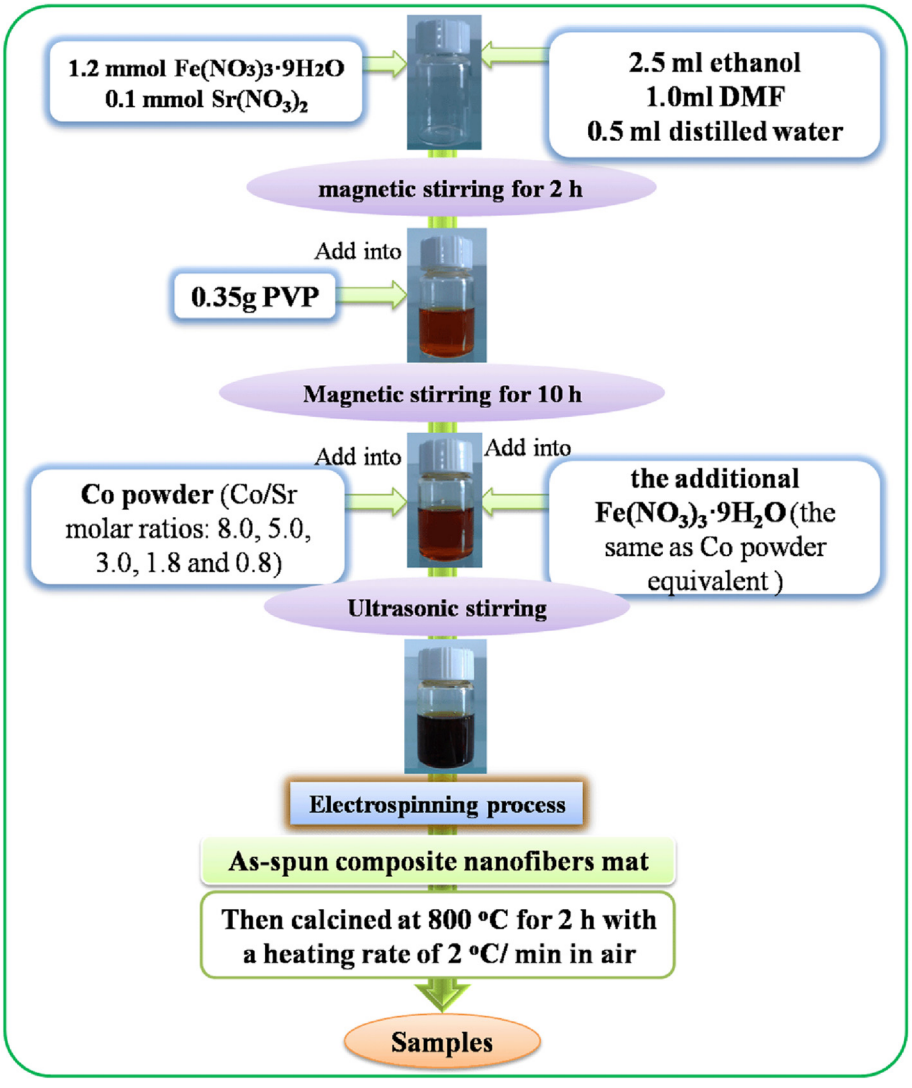

Figure 1 The graph of experimental flow.

stirring for 2 h. Then, 0.35 g of poly (vinyl pyrrolidone) (PVP; M_w = 1,300,000) was dissolved in the above solution and stirred for 10 h at room temperature to form a homogeneous viscous solution. Subsequently, the Co powder (Sinopharm Chemical Reagent Co., Ltd., Shanghai, China, 99%, 200 mesh) was dispersed ultrasonically in the PVP/nitrate solution with different Co/Sr^{2+} molar ratios (8.0, 5.0, 3.0, 1.8, and 0.8). And the additional equivalent $Fe(NO_3)_3 \cdot 9H_2O$ was also added into the above solution to form the resultant precursor. The electrospinning process was performed at a voltage of 13.5 kV DC, with a 15-cm spacing between the needle tip and the collector, and a feed rate of 0.3 ml/h was pumped by a syringe pump. Finally, the as-electrospun nanofibers were collected and annealed at 800°C for 2 h with a heating rate of 2°C/min in air and then cooled naturally to room temperature.

X-ray diffraction (XRD) patterns were recorded by a PANalytical diffractometer (PANalytical B.V., Almelo, The Netherlands) using Cu Kα radiation. Field emission scanning electron microscopy (FE-SEM; Hitachi S-4800, Hitachi, Ltd., Chiyoda, Tokyo, Japan) and transmission electron microscopy (TEM; Tecna™ G^2F30, FEI Co., Hillsboro, OR, USA) equipped with energy-dispersive X-ray analysis (EDX; Oxford Instruments, Abingdon, Oxfordshire, UK) were used to characterize the microstructure of the samples. The magnetic hysteresis loops were measured by a vibrating sample magnetometer (VSM; MicroSense EV9, MicroSense, LLC, Lowell, MA, USA) at room temperature with a maximum applied field of 20 kOe.

Results and discussion

As shown in Figure 2, SEM images clearly exhibit the morphologies of $CoFe_2O_4/SrFe_{12}O_{19}$ nanofibers with different Co/Sr^{2+} molar ratios (8.0, 5.0, 3.0, 1.8, and 0.8). Continuously linear structure and uniform diameter can be seen in all annealed nanofibers after the PVP was removed. And the diameter of these nanofibers ranged from 200 to 350 nm. When the Co/Sr^{2+} molar ratio is higher than 5.0, the nanofiber surface is smooth in Figure 2a,b. Decreasing the Co/Sr^{2+} molar ratio, the nanofibers possess a slightly rough surface and hollow structure. It indicated that the crystallite of the nanofibers grow up with the increase of Sr^{2+}.

The crystal structure of the samples is investigated by XRD technique, and the patterns are shown in Figure 3. For the samples with Co/Sr^{2+} molar ratio of 8.0 and 5.0, only the diffraction peaks of $CoFe_2O_4$ rather than $SrFe_{12}O_{19}$ are found because the Sr^{2+} ratios in their precursors are low. It seems that the diffraction peaks of $SrFe_{12}O_{19}$ begin to appear when the Co/Sr^{2+} molar ratio is 3.0, and they become narrower and stronger with the advance of Sr^{2+} ions. When the Co/Sr^{2+} molar ratio is 1.8, the diffraction intensities of $CoFe_2O_4$ phase and $SrFe_{12}O_{19}$ phase are approximately equal. Furthermore, the content of $CoFe_2O_4$ reduces while that of $SrFe_{12}O_{19}$ increases with the decrease of Co/Sr^{2+} molar ratio. Regarding the formation of $CoFe_2O_4/SrFe_{12}O_{19}$ nanofibers, the possible chemical reactions during the sintering process are inferred as follows:

$$Fe(NO_3)_3 \rightarrow Fe_2O_3 + NO_x$$
$$Sr(NO_3)_2 \rightarrow SrO + NO_x$$
$$SrO + CO_2 \rightarrow SrCO_3$$
$$SrCO_3 + Fe_2O_3 \rightarrow SrFe_2O_4 + CO_2$$
$$SrFe_2O_4 + 5Fe_2O_3 \rightarrow SrFe_{12}O_{19}\ [23]$$
$$2Co + O_2 \rightarrow 2CoO$$
$$CoO + Fe_2O_3 \rightarrow CoFe_2O_4\ [18]$$

Furthermore, the average crystallite size of $CoFe_2O_4$ and $SrFe_{12}O_{19}$ were calculated using the Scherrer equation ($L = K\lambda/\beta \cos\theta$, where λ is the X-ray wavelength in nanometer (nm), β is the full width at half maximum (FWHM) of diffraction peak, and K is a constant related to crystallite shape, normally taken as 0.89 [24]), and the

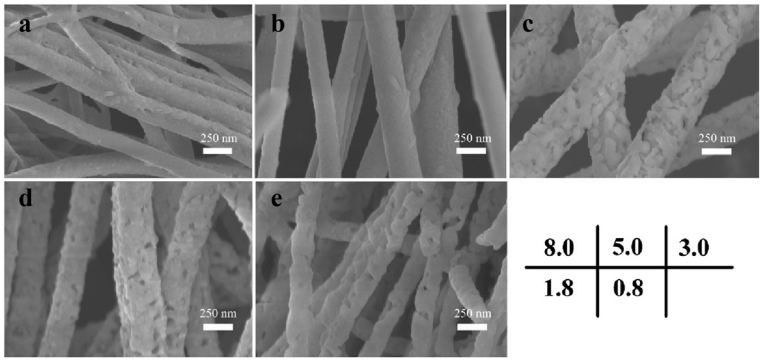

Figure 2 SEM images of $CoFe_2O_4/SrFe_{12}O_{19}$ nanofibers with different Co/Sr^{2+} molar ratios: (a) 8.0, (b) 5.0, (c) 3.0, (d) 1.8, and (e) 0.8.

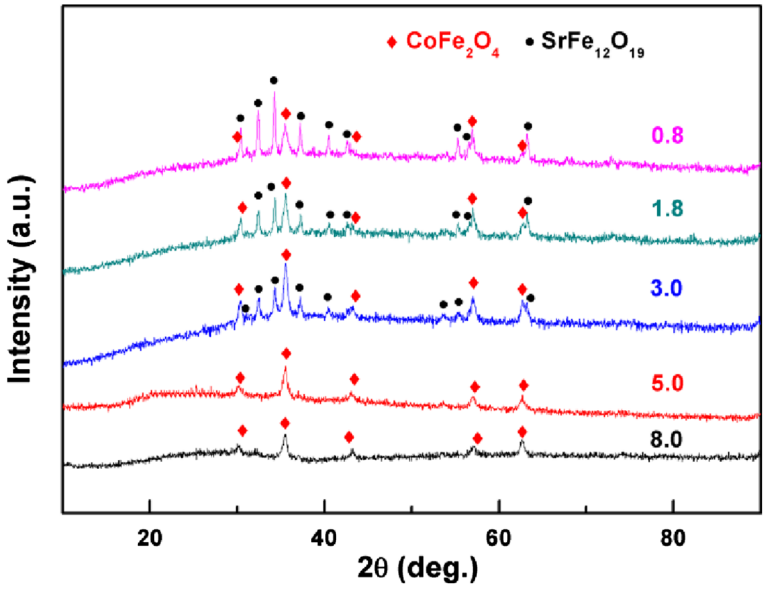

Figure 3 XRD patterns of $CoFe_2O_4/SrFe_{12}O_{19}$ nanofibers with different Co/Sr^{2+} molar ratios.

values are listed in Table 1. With the Co/Sr^{2+} molar ratio changing from 3.0 to 0.8, the crystallite size of $SrFe_{12}O_{19}$ increases from 26 to 29 nm, but that of $CoFe_2O_4$ was basically equal to about 17 nm. Therefore, the increase of Sr^{2+} ions, meaning to increase the $SrFe_{12}O_{19}$ content, leads to the increase of the average crystallite size of the nanofiber.

The representative TEM images of the $CoFe_2O_4/SrFe_{12}O_{19}$ nanofibers with the Co/Sr^{2+} molar ratio of 1.8 are presented in Figure 4a,b; they show a continuously linear structure and uniform diameter, which is corresponding to the above SEM observation (Figure 2). It is easily seen that the nanofibers consisted of two sizes of grains: one looks like hexagonal plate type structure $SrFe_{12}O_{19}$ and another is cubical $CoFe_2O_4$. Contrasting to the result of the average crystallite size calculated by XRD, the crystallite size is smaller than the grain obtained by TEM, so we do not make sure that every grain is single crystalline. Compared with the sample in Figure 4b, the $CoFe_2O_4/SrFe_{12}O_{19}$ nanofibers with a Co/Sr^{2+} molar ratio of 8.0 in Figure 4e present a smoother surface, and the grains are smaller than the other samples. As shown in Figure 4e, the nanofibers are composed of uniform grains, and the grains densely stacked along the direction of nanofiber axis.

Table 1 Average crystallite size of the samples with different Co/Sr^{2+} molar ratios

Molar ratio (Co/Sr^{2+})	$D_{SrFe_{12}O_{19}}$ (nm)	$D_{CoFe_2O_4}$ (nm)
8.0	/	17
5.0	/	17
3.0	26	18
1.8	27	18
0.8	29	16

A high-resolution TEM image of the area is marked by red square in Figure 4b; as shown in Figure 4c, the interplanar spacing is measured to be 0.21 nm, which is consistent with the (206) crystallographic orientation of M-type hexagonal $SrFe_{12}O_{19}$. And another interplanar spacing is measured to be 0.25 nm, corresponding to the separation between the (113) lattice planes of $CoFe_2O_4$. The EDX spectrum of the nanofibers are shown in Figure 4d,f, confirming the presence of Fe, O, Sr, and Co in the samples, which is in good agreement with the mentioned result of XRD in Figure 3. So, it can be inferred that $SrFe_{12}O_{19}$ phase also exist in the samples with Co/Sr^{2+} molar ratio of 5.0 and 8.0. But the $SrFe_{12}O_{19}$ phase cannot be observed by corresponding XRD due to the tiny Sr element contents in these samples.

Figure 5a shows the magnetic hysteresis loops of the nanofibers measured with a VSM at room temperature. The results demonstrate a good single-phase magnetic behavior, and the magnetization changes smoothly with the applied field, which suggest that the soft and hard magnetic phase exchange coupled strongly [8,25].

The tendency of M_s and H_c of the samples versus Co/Sr^{2+} molar ratios is illustrated in Figure 5b. It is observed that the M_s increases monotonously and reaches to the maximum value of 62.8 emu/g corresponding to

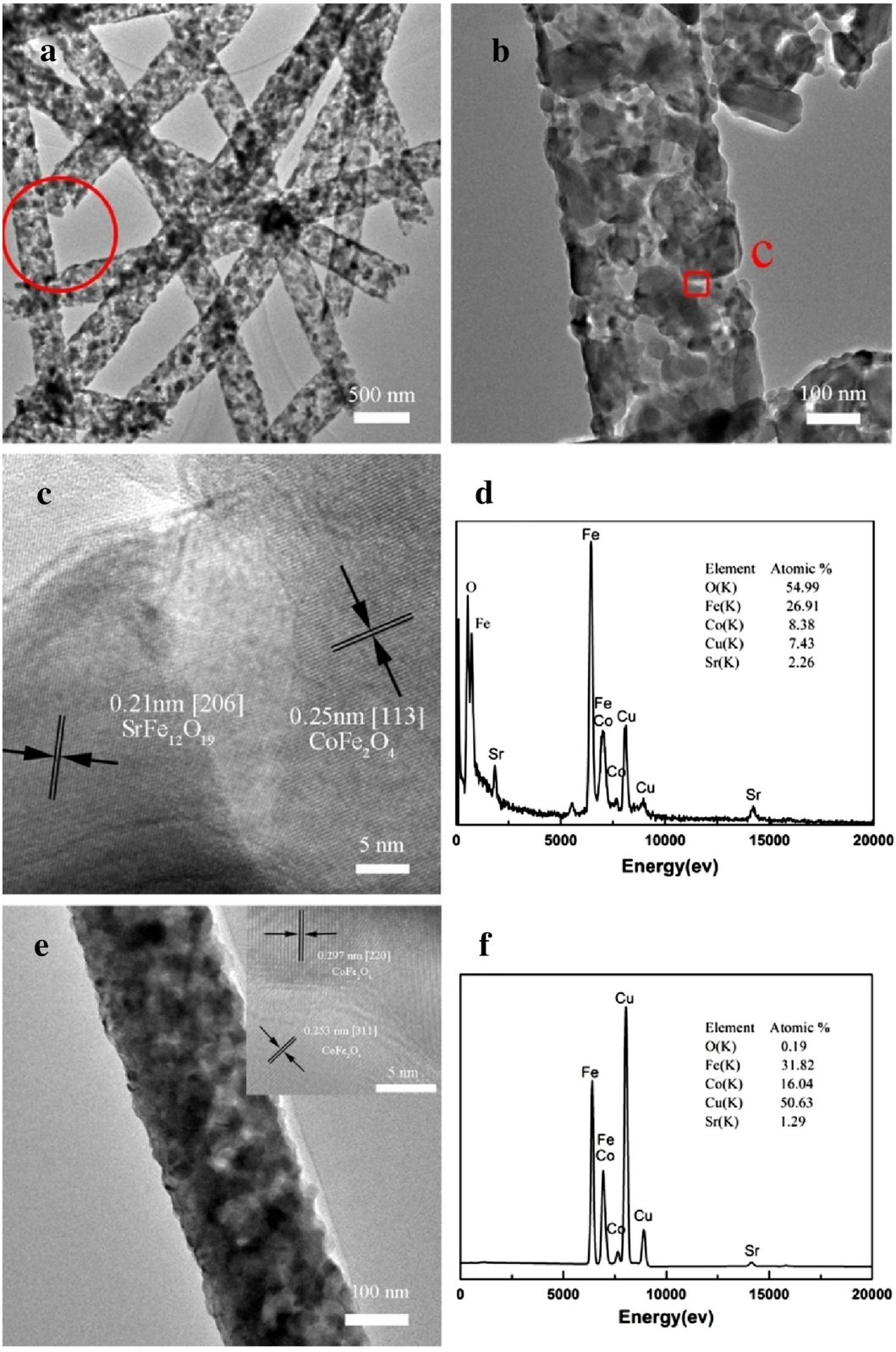

Figure 4 TEM and HRTEM images and EDX spectrum of $CoFe_2O_4/SrFe_{12}O_{19}$ nanofibers. TEM images **(a, b)**, HRTEM image **(c)**, and EDX spectrum **(d)** of $CoFe_2O_4/SrFe_{12}O_{19}$ nanofibers with a Co/Sr^{2+} molar ratio of 1.8. TEM image **(e)**, top left inset in (e) showing a HRTEM pattern, and EDX spectrum **(f)** of $CoFe_2O_4/SrFe_{12}O_{19}$ nanofibers with a Co/Sr^{2+} molar ratio of 8.0.

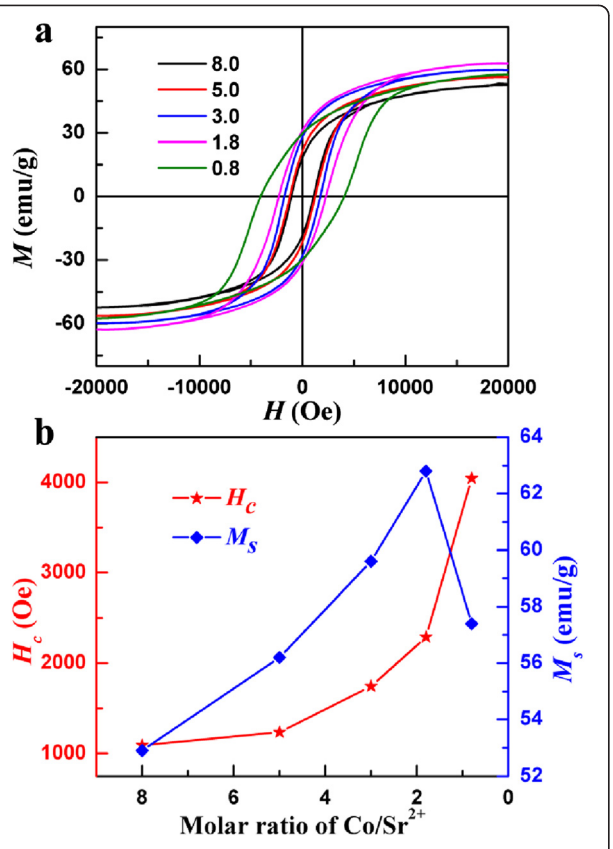

Figure 5 Magnetic hysteresis loops and tendency of M_s and H_c of the samples. (a) Magnetic hysteresis loops of the samples with different Co/Sr^{2+} molar ratios. **(b)** The tendency of M_s and H_c of the samples with different Co/Sr^{2+} molar ratios.

the sample with the Co/Sr^{2+} molar ratio of 1.8. Subsequently, the M_s decrease drastically with the further decrease of the Co/Sr^{2+} molar ratios. The corresponding H_c values increase monotonously with the decrease of the Co/Sr^{2+} molar ratios in Figure 5b. This may be due to the fact that $SrFe_{12}O_{19}$ possesses a bigger magnetocrystalline anisotropy, and the magnetizations are mainly determined by the exchange coupling interaction between the soft and hard phases with increasing Sr^{2+} [26].

Table 2 The part parameters of magnetic performances of $CoFe_2O_4/SrFe_{12}O_{19}$ nanocomposite nanofibers

Co/Sr molar ratio	M_s (emu/g)	M_r (emu/g)	M_r/M_s	$(BH)_{max}$ (MG Oe)
8.0	52.90	18.22	0.34	0.36
5.0	56.20	21.50	0.38	0.47
3.0	59.6	28.10	0.47	0.91
1.8	62.8	31.21	0.50	1.29
0.8	57.4	29.80	0.52	2.20

And the parameters of the remanent magnetization M_r, squareness M_r/M_s, and the energy product of the nanofibers are shown in Table 2.

It is well known that the exchange coupling interaction and dipolar interaction play a major role to determine the magnetic properties of the magnetic nanocomposite materials. There exist three different models of exchange coupling interaction formed at the interface between soft-soft, hard-hard, and soft-hard grains, which has been proposed by Han et al. in 2004 [27]. The sufficient exchange coupling will not only arrange the magnetization in the $CoFe_2O_4$ grains but also make the magnetic moments of the interface of the $CoFe_2O_4/SrFe_{12}O_{19}$ nanocomposite deviating from the local easy axis and aligning in parallel with each other, which leads to a higher value of the M_s [28]. The coercivity of the samples increased from 1,089 to 4,046 Oe continuously, which is owing to the high H_k of $SrFe_{12}O_{19}$ nanofibers. And with increasing ratio of $SrFe_{12}O_{19}$, the exchange coupling interactions between the hard/soft magnetic phases are enhanced, and the H_c and M_s all increased.

Simultaneously, the influence of crystallite size on the H_c and M_s is displayed as follows. The theoretical calculation suggests that the critical dimension of the soft phase (t_s) in the hard/soft composite materials should be less than twice of the domain wall width (δ_ω) of the hard phase for a perfect demagnetization of hard/soft phases [29], and the domain wall width of the $SrFe_{12}O_{19}$ is approximately 9 nm [30]. And another theoretical calculation indicates that the critical size of both phases should be about equal [31]. An optimal value of the crystallite size of the hard and soft phases results in the maximum of M_s. While the value of the Co/Sr^{2+} was 0.8, the average crystallite size of the $CoFe_2O_4$ and $SrFe_{12}O_{19}$ has a wide difference, which leads to a decrease in M_s. The comparison of the magnetic properties, morphologies, and annealing temperature between the results of the $CoFe_2O_4/SrFe_{12}O_{19}$ nanocomposites is published by previous literatures. The higher M_s was obtained in this work in a lower annealing temperature. The H_c was moderate because of lower Sr^{2+} content compared with other articles. The details of parameters of performances are listed in Table 3.

Conclusions

$CoFe_2O_4/SrFe_{12}O_{19}$ nanofibers were fabricated by electrospinning and calcination process. Simultaneously, a novel way that cobalt powder was used in the precursor sol-gel instead of cobalt salt was adopted in this work. What is more, the samples had an enhanced saturation magnetization of 62.8 emu/g and coercivity of 2,290 Oe when the average crystallite size of the hard/soft phases reached up to an optimal value. And the hard/soft

Table 3 The comparison of the properties between the $CoFe_2O_4/SrFe_{12}O_{19}$ nanocomposites prepared by electrospinning and other methods

Preparation method	M_s (emu/g)	H_c (Oe)	Structure	Annealing temperature	Reference
Coprecipitation	27.9	3,567	Core-shell nanoparticle	800°C	[15]
Modified flux method	50	1,798	Nanoparticle	900°C	[14]
Coprecipitation	42.5	2,475	Nanoparticle	1,000°C	[16]
Electrospinning	60.9	3,190	Nanofibers	900°C	Our group [9]
Electrospinning	62.8	2,290	Nanofibers	800°C	This work

magnetic nanocomposite exhibited a strong exchange coupling interaction.

Competing interests
The authors declare that they have no competing interests.

Authors' contributions
LP designed and carried out the experiments and wrote the paper. DC and PJ participated in the study preparation, characterization of morphologies, and measurement of magnetic properties of the nanofibers. JW and QL supervised the whole study. All authors read and approved the final manuscript.

Authors' information
QL and JW are professors at the Key Laboratory for Magnetism and Magnetic Materials of the Ministry of Education, Lanzhou University. LNP is an M.S. student.

Acknowledgements
This work is supported by the National Science Fund of China (51171075, 51371092) and the Fundamental Research Funds for the Central Universities (lzujbky-2013-32).

Received: 2 December 2014 Accepted: 17 February 2015
Published online: 14 March 2015

References
1. Rakshit R, Mandal M, Pal M, Mandal K. Tuning of magnetic properties of $CoFe_2O_4$ nanoparticles through charge transfer effect. Appl Phys Lett. 2014;104:092412–0912417.
2. Wang Y, Su D, Ung A, Ahn JH, Wang G. Hollow $CoFe_2O_4$ nanospheres as a high capacity anode material for lithium ion batteries. Nanotechnology. 2012;23:305501–7.
3. Mazuera D, Perales O, Suarez M, Singh S. Synthesis, characterization and thermal analysis of polyimide–cobalt ferrite nanocomposites. Mater Sci Eng A. 2010;527:6393–9.
4. Lopez-Ortega A, Estrader M, Alvarez GA, Roca AG, Nogues J. Applications of exchange coupled bi-magnetic hard/soft and soft/hard magnetic core/shell nanoparticles. Phys Rep. 2015;553:1–32.
5. Xi L, Wang Z, Zuo Y, Shi X. The enhanced microwave absorption property of CoFe2O4 nanoparticles coated with a Co3Fe7–Co nanoshell by thermal reduction. Nanotechnology. 2011;22:045707.
6. Mazario E, Herrasti P, Morales MP, Menendez N. Synthesis and characterization of $CoFe_2O_4$ ferrite nanoparticles obtained by an electrochemical method. Nanotechnology. 2012;23:355708.
7. Santi Masensiri MS. Nanostructures and magnetic properties of cobalt ferrite (CoFe2O4) fabricated by electrospinning. Appl Phys A. 2009;97:167–77.
8. Liu W, Chan Y, Cai J, Leung C, Mak C, Wong K, et al. Understanding the formation of ultrafine spinel CoFe2O4 nanoplatelets and their magnetic properties. J Appl Phys. 2012;112:104306.
9. Radmanesh MA, Seyyed Ebrahimi SA, Yourdkhani A, Khanmohammadi H. Investigation of magnetic interactions in core/shell structured $SrFe_{12}O_{19}/NiZnFe_2O_4$ nanocomposite. J Supercond Nov Magn. 2011;25:2757–62.
10. Tyagi S, Baskey HB, Agarwala RC, Agarwala V, Shami TC. Development of hard/soft ferrite nanocomposite for enhanced microwave absorption. Ceram Int. 2011;37:2631–41.
11. Lu X, Wang C, Wei Y. One-dimensional composite nanomaterials: synthesis by electrospinning and their applications. Small. 2009;5:2349–70.
12. Liu F, Zhu J, Yang W, Dong Y, Hou Y, Zhang C, et al. Building nanocomposite magnets by coating a hard magnetic core with a soft magnetic shell. Angew Chem Int Ed. 2014;53:2176–80.
13. Dong J, Zhang Y, Zhang X, Liu Q, Wang J. Improved magnetic properties of $SrFe_{12}O_{19}$/FeCo core–shell nanofibers by hard/soft magnetic exchange–coupling effect. Mater Lett. 2014;120:9–12.
14. Hue DTM, Lampen P, Manh TV, Viet VD, Chinh HD, Srikanth H, et al. Synthesis, structure, and magnetic properties of $SrFe_{12}O_{19}$/La1 – xCaxMnO3 hard/soft phase composites. J Appl Phys. 2013;114:123901–7.
15. Gu FM, Pan WW, Liu QF, Wang JB. Electrospun magnetic $SrFe_{12}O_{19}$ nanofibres with improved hard magnetism. J Phys D-Appl Phys. 2013;46:445003–10.
16. Wang J, Zeng C. Growth of $SrFe_{12}O_{19}$ nanowires under an induced magnetic field. J Cryst Growth. 2004;270:729–33.
17. Shen X, Liu M, Song F, Meng X. Structural evolution and magnetic properties of $SrFe_{12}O_{19}$ nanofibers by electrospinning. J Sol–gel Sci Techn. 2009;53:448–53.
18. Sachin Tyagi HBB, Agarwala RC, Agarwala V, Shami TC. Reaction kinetic, magnetic and microwave absorption studies of SrFe12O19/CoFe2O4 ferrite nanocrystals. T Indian I Metals. 2011;64:271–7.
19. Xie T, Xu L, Liu C. Synthesis and properties of composite magnetic material $SrCo_xFe_{12-x}O_{19}$ (x = 0–0.3). Powder Technol. 2012;232:87–92.
20. Moyet RP, Cardona Y, Vargas P, Silva J, Uwakweh ONC. Coercivity and superparamagnetic evolution of high energy ball milled (HEBM) bulk $CoFe_2O_4$ material. Mater Charact. 2010;61:1317–25.
21. Li D, Xia Y. Electrospinning of nanofibers: reinventing the wheel? Adv Mater. 2004;16:1151–70.
22. Zhang L, Li Z. Synthesis and characterization of $SrFe_{12}O_{19}/CoFe_2O_4$ nanocomposites with core-shell structure. J Alloy Compd. 2009;469:422–6.
23. Nga TTV, Duong NP, Loan TT, Hien TD. Key step in the synthesis of ultrafine strontium ferrite powders ($SrFe_{12}O_{19}$) by sol–gel method. J Alloy Compd. 2014;610:630–4.
24. Monshi A. Modified Scherrer equation to estimate more accurately nano-crystallite size using XRD. WJNSE. 2012;02:154–60.
25. Roy D, Shivakumara C, Anil Kumar PS. Observation of the exchange spring behavior in hard–soft-ferrite nanocomposite. J Magn Magn Mater. 2009;321:L11–4.
26. Xiang J, Zhang X, Li J, Chu Y, Shen X. Fabrication, characterization, exchange coupling and magnetic behavior of $CoFe_2O_4/CoFe_2$ nanocomposite nanofibers. Chem Phys Lett. 2013;576:39–43.
27. Han GB, Gao RW, Fu S, Feng WC, Liu HQ, Chen W, et al. Effective anisotropy between magnetically soft and hard grains in nanocomposite magnets. Appl Phys A. 2004;81:579–82.
28. Song F, Shen X, Liu M, Xiang J. Microstructure, magnetic properties and exchange–coupling interactions for one-dimensional hard/soft ferrite nanofibers. J Solid State Chem. 2012;185:31–6.
29. Skomski R, Coey J. Giant energy product in nanostructured two-phase magnets. Phys Rev B. 1993;48:15812–6.
30. Garcia-Casillas P. Remanence properties of barium hexaferrite. J Alloy Compd. 2004;369:185–9.
31. Kneller EF, Member Z, Hawig R. The exchange-spring magnet: a new material principle for permanent magnets. IEEE Trans Magn. 1991;27:3588–600.